Since January 2020 Elsevier has created a COVID-19 resource centre with free information in English and Mandarin on the novel coronavirus COVID-19. The COVID-19 resource centre is hosted on Elsevier Connect, the company's public news and information website.

Journal of Virological Methods 286 (2020) 113979

Contents lists available at ScienceDirect

Journal of Virological Methods

journal homepage: www.elsevier.com/locate/jviromet

High-throughput viral microneutralization method for feline coronavirus using image cytometry

Morgan Pearson [a], Alora LaVoy [a], Leo Li-Ying Chan [b,*], Gregg A. Dean [a]

[a] Department of Microbiology, Immunology, and Pathology, Colorado State University, Fort Collins, CO, 80523, United States
[b] Department of Advanced Technology R&D, Nexcelom Bioscience LLC, Lawrence, MA, 01843, United States

ARTICLE INFO

Keywords:
Feline coronavirus (FCoV)
Viral titer
Plaque-Reduction neutralization tests (PRNT)
High-throughput screening (HTS)
Image cytometry
Celigo

ABSTRACT

Feline coronaviruses (FCoV) are members of the alphacoronavirus genus that are further characterized by serotype (types I and II) based on the antigenicity of the spike (S) protein and by pathotype based on the associated clinical conditions. Feline enteric coronaviruses (FECV) are associated with the vast majority of infections and are typically asymptomatic. Within individual animals, FECV can mutate and cause a severe and usually fatal disease called feline infectious peritonitis (FIP), the leading infectious cause of death in domestic cat populations. There are no approved antiviral drugs or recommended vaccines to treat or prevent FCoV infection. The plaque reduction neutralization test (PRNT) traditionally employed to assess immune responses and to screen therapeutic and vaccine candidates is time-consuming, low-throughput, and typically requires 2–3 days for the formation and manual counting of cytolytic plaques. Host cells are capable of carrying heavy viral burden in the absence of visible cytolytic effects, thereby reducing the sensitivity of the assay. In addition, operator-to-operator variation can generate uncertainty in the results and digital records are not automatically created. To address these challenges we developed a novel high-throughput viral microneutralization assay, with quantification of virus-infected cells performed in a plate-based image cytometer. Host cell seeding density, microplate surface coating, virus concentration and incubation time, wash buffer and fluorescent labeling were optimized. Subsequently, this FCoV viral neutralization assay was used to explore immune correlates of protection using plasma from naturally FECV-infected cats. We demonstrate that the high-throughput viral neutralization assay using the Celigo Image Cytometer provides a robust and efficient method for the rapid screening of therapeutic antibodies, antiviral compounds, and vaccines. This method can be applied to various viral infectious diseases to accelerate vaccine and antiviral drug discovery and development.

1. Introduction

Feline coronaviruses (FCoV), present in most domestic cat populations worldwide, are members of the alphacoronavirus genus that are further characterized by serotype (type I and II) based on the antigenicity of their spike (S) proteins (An et al., 2011; Kummrow et al., 2005; Li, 2016; Pratelli, 2008). More recently, designation as clade A or B based on the sequence and biological properties of S protein has been proposed and would correlate with FCoV type I and II viruses, respectively (Whittaker et al., 2018). Viruses from both types and clades are additionally characterized by distinct pathotypes based on the associated clinical conditions. Feline enteric coronaviruses (FECV) are associated with the vast majority of infections and are typically asymptomatic or present as a mild enteropathy. Within individual animals, FECV can mutate and cause a severe and usually fatal disease called feline infectious peritonitis (FIP). FIP is the leading infectious cause of death in domestic cats (Hartmann, 2005), affecting 7.8 to 12% of seropositive kittens every year (Addie et al., 2009; Rohrbach et al., 2001). Currently, there are no approved antiviral drugs or recommended vaccines to treat or prevent FCoV, although recent reports provide some promise (Addie et al., 2020; Dickinson et al., 2020; Pedersen, 2014a, b; Pedersen et al., 2019; Takano et al., 2020).

The complex and variable pathogenesis of FIP has been studied for decades. The clinical presentation, often vague, consists of fever, weight loss, and depression. Diagnosis can be difficult and is based on a preponderance of evidence as there is no single definitive ante mortem test (Felten and Hartmann, 2019). Histological lesions are characterized by granulomatous inflammation and vasculitis that may or may not result

* Corresponding author.
E-mail address: lchan@nexcelom.com (L.L.-Y. Chan).

https://doi.org/10.1016/j.jviromet.2020.113979
Received 2 June 2020; Received in revised form 12 July 2020; Accepted 19 September 2020
Available online 23 September 2020

in proteinaceous effusions in body cavities. Neurologic symptoms with associated inflammatory lesions in the central nervous system are also relatively common (Foley et al., 1998). The complexity of the virus itself along with the variability of the clinical manifestation has confounded efforts to determine immune correlates of protection that should be targeted with vaccine strategies. We recently reported that control of FECV replication in naturally infected cats was associated with mucosal and systemic antibody responses while cell-mediated responses were minimally apparent (Pearson et al., 2019). Therefore, assays to determine effector functions of antibodies will be crucial for the development and evaluation of a successful vaccine.

Traditionally, plaque-reduction neutralization tests (PRNT) have been the preferred neutralization assays involving FCoV (Shiba et al., 2007). In PRNT assays, plasma or serum is first mixed with infectious virus. After incubation, the mixture is added to susceptible host cells and incubated until cytopathic effects (CPE) appear. Subsequently, the host cells are fixed and stained with crystal violet to reveal the FCoV infected plaques. Previously, FCoV neutralizing antibodies have shown approximately 75% or more plaque reduction (Shiba et al., 2007). The PRNT assay for FCoV is time-consuming, requiring up to 2–3 days for the formation of cytolytic plaques (Supplementary Fig. 1). Additionally, the host cells are capable of carrying heavy viral burden in the absence of visible cytolytic effects, making it extremely difficult to manually count accurately in bright field (Masci et al., 2019). Manual plaque counting is low-throughput and has operator-to-operator variation, and digital records are not always captured (Masci et al., 2019). Therefore, it is crucial to develop improved methods for high-throughput measurement of viral infection and neutralization.

Recent advancements in image cytometry systems have enabled the development of novel high-throughput cell-based assays performed directly in standard 6- to 1536-well microplates (Jorquera et al., 2019; Masci et al., 2019; Shambaugh et al., 2017; Yang et al., 2017). The Celigo Image Cytometer has demonstrated automated enumeration of viral plaques, foci, and individual virus-infected cells in 96-well microplates using bright field or fluorescence imaging in less than 5 or 10 min, respectively, which can significantly reduce the time required for counting and analysis as well as eliminate operator-to-operator variation (Ramos et al., 2019; Rosen et al., 2019; Viedma and Pickett, 2018). Furthermore, it has been shown that fluorescence detection of plaques, foci, or individual infected cells via immunostaining or fluorescent protein reporter can be detected earlier than the traditional cytolytic plaques, where assay time duration can be effectively reduced by 40% (Masci et al., 2019).

In this work, we developed a high-throughput FCoV microneutralization assay employing the Celigo Image Cytometer for rapid quantification of virus-infected cells. Multiple parameters were optimized including host cell seeding density, microplate surface coating, virus concentration and incubation time, fluorescent labeling, and assay buffers. The optimized assay was employed to test feline plasma for the presence of FCoV-neutralizing antibodies. The proposed high-throughput viral microneutralization assay using Celigo Image Cytometer provides a robust and efficient method for virologists to quickly identify potential therapeutic antibodies or antiviral compounds for various viral infectious diseases, which could have a significant impact on efficiency of drug discovery and vaccine development.

2. Materials and methods

2.1. Host cell preparation

CRFK (CCL-94, ATCC, Manassas, VA), an adherent epithelial cell line derived from feline kidney cortex, were cultured in DMEM (15−013-CV, Corning, Corning, NY) supplemented with 10% FBS, 1% penicillin/streptomycin mixture (17−602E, Lonza, Morristown, NJ), 2 mM Corning glutagro, and 15 mM HEPES at 37 °C and 5% CO_2. Approximately 6000 cells per well were plated in a sterile black-walled 96-well microplate with μCLEAR well bottoms (655956, Greiner Bio-One, Monroe, NC) with 200 μL medium per well. The cells were allowed to adhere to the plate overnight at 37 °C for the infectivity and neutralization assays.

2.2. Feline coronavirus preparation

Feline coronavirus strain FCoV-WSU-79–1146 was generously provided by Dr. Niels Pedersen (University of California, Davis) (Herrewegh et al., 1998). CRFK cells were added to a collagen type I-coated T-75 flask (658950-005, Greiner Bio-One) and incubated for 24 h. The medium was then removed and the cells were washed with Dulbecco's phosphate buffered saline (DPBS, SH30264.FS, GE Healthcare, Chicago, IL). An untitered stock of FCoV-WSU- 79-1146 type II virus was first diluted 1:25 in DPBS and then added to the cells and incubated for 1 h at 37 °C. Next, the viral inoculum was removed and the cells were washed 2X with DPBS. Subsequently, culture medium was added and cells were incubated for 48 h. The supernatant was collected into a 15-mL tube, centrifuged for 10 min at 250 x g, aliquoted and stored at −80 °C for single use. CRFK infections in 96-well plates followed the same method unless noted.

2.3. Fluorescent staining of infected host cells

CRFK infected with FCoV-WSU- 79-1146 were washed with 200 μL of DPBS per well, and then fixed by adding 100 μL of 4% paraformaldehyde (15714-S, Electron Microscopy Sciences, Hatfield, PA) in 1X PBS (21-040-CV, Corning) per well. The cells were incubated at room temperature (RT) for 30 min and washed 2X with 200 μL of DPBS. The fixed host cells were then permeabilized by adding 100 μL of 0.1% Triton X-100 to each well and incubating for 5 min at RT. Subsequently, the wells were washed 2X with 200 μL of DPBS and blocked for 30 min at RT by adding 200 μL of 0.45 μm-filtered (229748, PES Syringe Filter, CELLTREAT Scientific Products, Pepperell, MA) 10% goat serum (SG-0500, Equitech-Bio, Kerrville, TX) in PBS. After the incubation, the blocking solution was replaced with 200 μL of DPBS.

Fluorescent labeling was performed at room temperature and plates were protected from light. All reagents were diluted in 3% filtered goat serum/PBS and used at 100 μL/well. The antibodies were diluted to 2 μg/mL and 0.45 μm-filtered. Primary monoclonal antibody recognizing feline coronavirus nucleocapsid protein (FIPV3-70, Custom Monoclonals International, Sacramento, CA) or isotype control antibody (clone MOPC-173, BioLegend, San Diego, CA) was added to the fixed cells and incubated for 1 h. Subsequently, the wells were washed 2X with 200 μL of DPBS. Next, Alexa Fluor 488 (AF488)-labeled goat anti-mouse IgG (H + L) secondary antibody (A32723, Thermo Fisher Scientific, Waltham, MA) was added and incubated for 1 h. The wells were again washed 2X with 200 μL of DPBS. Finally, 1 μg/mL of DAPI nuclear stain (MBD0015, MilliporeSigma, St. Louis, MO) was added and incubated for 7 min. The wells were washed 2X with 200 μL of DPBS, and a final volume of 100 μL of DPBS was added to each well prior to image cytometry analysis.

2.4. Celigo image cytometer

The Celigo Image Cytometer utilizes one bright field (BF) and four fluorescence (FL) imaging channels: Blue (EX: 377/50 nm, EM: 470/22 nm), Green (EX: 483/32 nm, EM: 536/40 nm), Red (EX: 531/40 nm, EM: 629/53 nm), and Far Red (EX: 628/40 nm, EM: 688/31 nm) with high-power light-emitting diodes to perform plate-based image cytometric analyses. It allows auto-focusing in each well based on the image contrast or the thickness of the bottom surface (Chan, 2020; Kessel et al., 2016; Zhang et al., 2017).

The Celigo software application "Confluence 1" was used to measure the host cell confluence percentages using the acquired bright field images. The preset ANALYZE parameters were optimized to

automatically calculate the area of host cells covering the well surface to determine the confluence percentages. The results were used to select optimal CRFK seeding density, as well as wash buffer and plate coating.

The Celigo software application "Target 1 + 2 + Mask" was used to identify the total number of DAPI-positive host cells in the Blue channel and quantify the percentages of green fluorescent infected cells. The Celigo instrument was set up to acquire images in the Target 1 (BF), Target 2 (Green), and Mask (Blue) channels, where the exposure times for Alexa Fluor 488 and DAPI were 400,000 and 450,000 μs, respectively. Hardware-based autofocus was used to focus in the BF channel, and the focus offsets were applied for the Green (+26 μm) and Blue (−5 μm) channels. The preset ANALYZE parameters were optimized to identify the DAPI-positive host cells above an intensity threshold of 4, then the gating feature was used to analyze the fluorescence intensities to determine AF488-positive infected cell population percentages. Image acquisition and analysis were performed simultaneously. In addition, the AF488 fluorescence intensities were measured to determine the optimal primary and secondary antibody concentrations for staining the infected host cells.

2.5. Host cell seeding density and incubation time optimization

CRFK seeding density was optimized so cells would reach high confluency by the end of the post-infection incubation. The number of cells seeded ranged from 3000 to 6000 cells per well in increments of 1000 and was tested in conjunction with growth time of 48 and 72 h (n = 4). At each time point, bright field images were acquired and analyzed using the image cytometer to automatically measure the confluence percentages of the host cells.

2.6. Fluorescent labeling optimization for detection of virus-infected cells

Immunostaining of FCoV-infected cells was optimized by testing antibody concentrations above and below manufacturer recommendations using cells infected with a 1:35 dilution of the viral stock. The primary antibody was tested at 0.25, 0.5, 1.0, and 2.0 μg/mL. The secondary antibody was tested at 0.5, 1.0, 2.0, and 4.0 μg/mL. After acquiring images of the infected cells using the image cytometer, the lowest concentrations that generated the highest signals with the lowest background were selected. The DAPI staining solution was used at 1.0 μg/mL following the manufacturer's protocol.

2.7. Optimal assay buffer and surface coating selection

DMEM and DPBS were compared for cellular retention during viral inoculation steps, as well as the virus diluent. Experimentation was performed by first seeding the wells of a 96-well plate with 6000 cells/well and allowing the cells to adhere for 24 h. DMEM and DPBS were then tested by washing half of the plate with 200 μL/well of DPBS and the other half with 200 μL/well of DMEM. Next, half of the plate was infected with 1:25 dilution of virus in DPBS and the other half was infected with 1:25 dilution of virus in DMEM. The rest of the infectivity assay and staining procedures were performed consistently (n = 4).

The experiment was performed with four microplate surface treatments, which were compared to determine their ability to promote optimal cell adhesion throughout infection and immunostaining. Samples of black-walled 96-well plates with μCLEAR well bottoms were provided by Greiner Bio-One (Kremsmünster, Austria): Advanced TC (655986), collagen type I (655956), poly-D-lysine (655946) and poly-L-lysine (655936). The plates were scanned and analyzed using the image cytometer under plate type Greiner 655087 in the software to measure the confluence percentages and infection rates.

Table 1
Characterizations of the 5 feline plasma samples.

	Plasma FCoV antibody	Fecal FCoV RNA	7-Month Observation
Feline #1	Positive	Negative	Plasma moved from positive to borderline
Feline #2	Positive	Positive	Always positive plasma and fecal FCoV RNA
Feline #3	Negative	Negative	Always negative plasma and fecal FCoV RNA
Feline #4	Positive	Negative	Fecal moved from positive to negative FCoV RNA
Feline #5	Negative	Negative	Always negative plasma and fecal FCoV RNA

2.8. Viral concentration and incubation time optimization

The viral supernatant inoculation concentration and incubation time were optimized to achieve the desired infection rate of 50–60%. Approximately 6000 CRFK cells were seeded into a 96-well plate (655956, Greiner Bio-One) for 24 h. Next, the host cells were infected with a serial dilution of infectious supernatant (1:10, 1:20, 1:40, 1:80, 1:160, 1:320, 1:640, 1:1280, 1:5120, 1:10240, and 1:20480) and post-inoculation incubation time points were analyzed at 24, 36, 48, and 72 h using image cytometry with fluorescent immunostaining (n = 4).

2.9. Plasma sample preparation

Cats were cared for in accordance with the Association for the

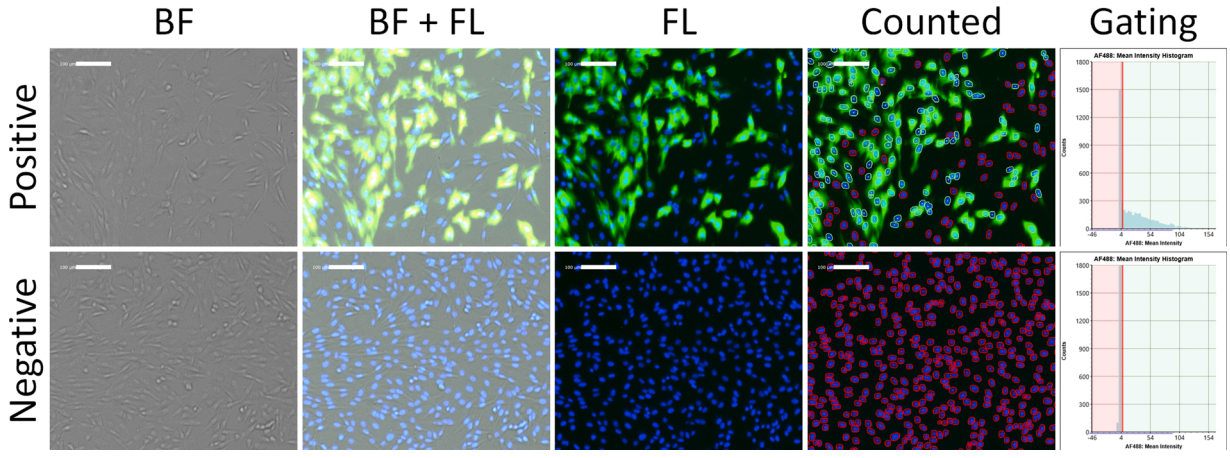

Fig. 1. Bright field and fluorescent images, and fluorescence intensity gating of positive and negative infection of CRFK cells using optimized scanning and analysis settings from image cytometry.

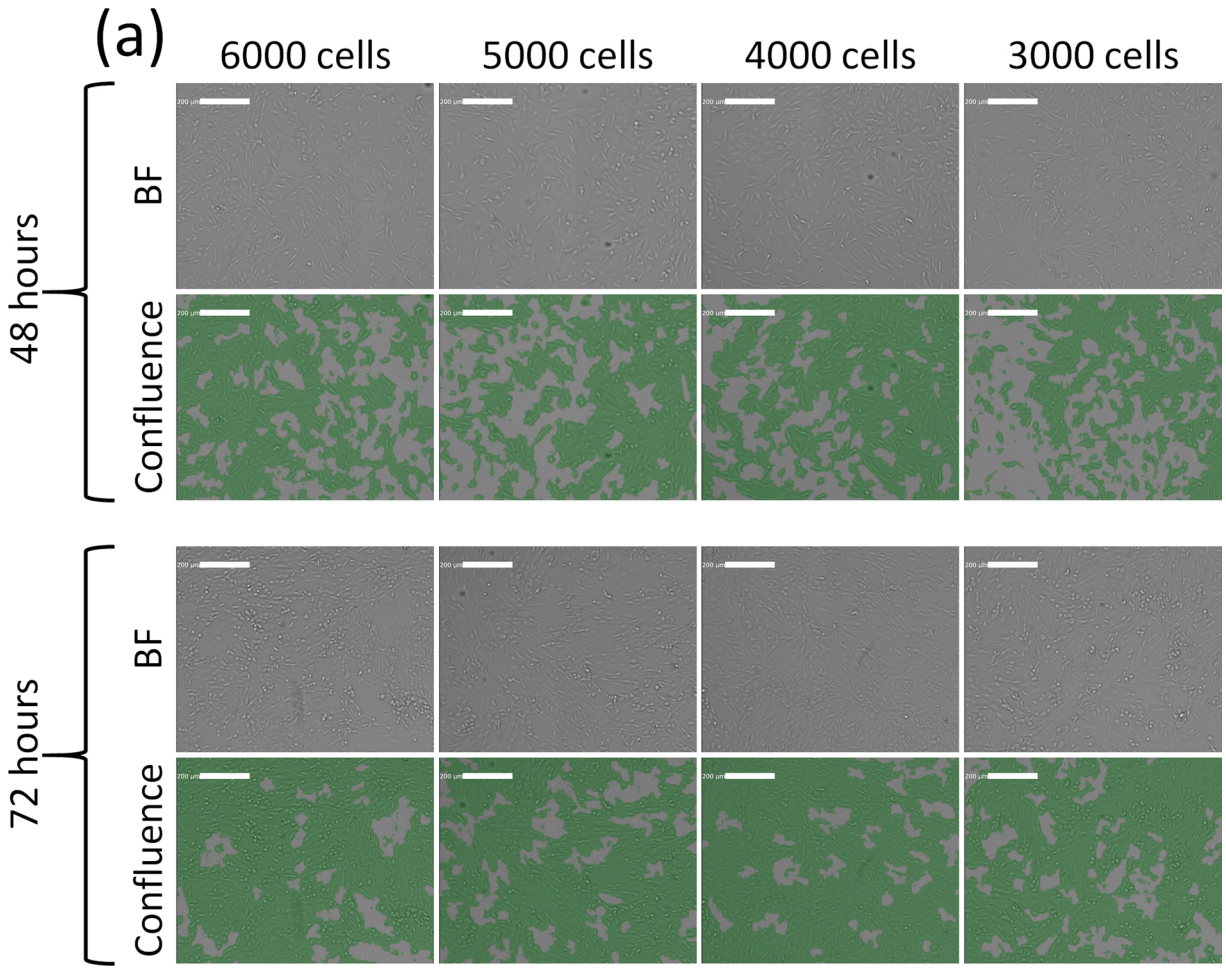

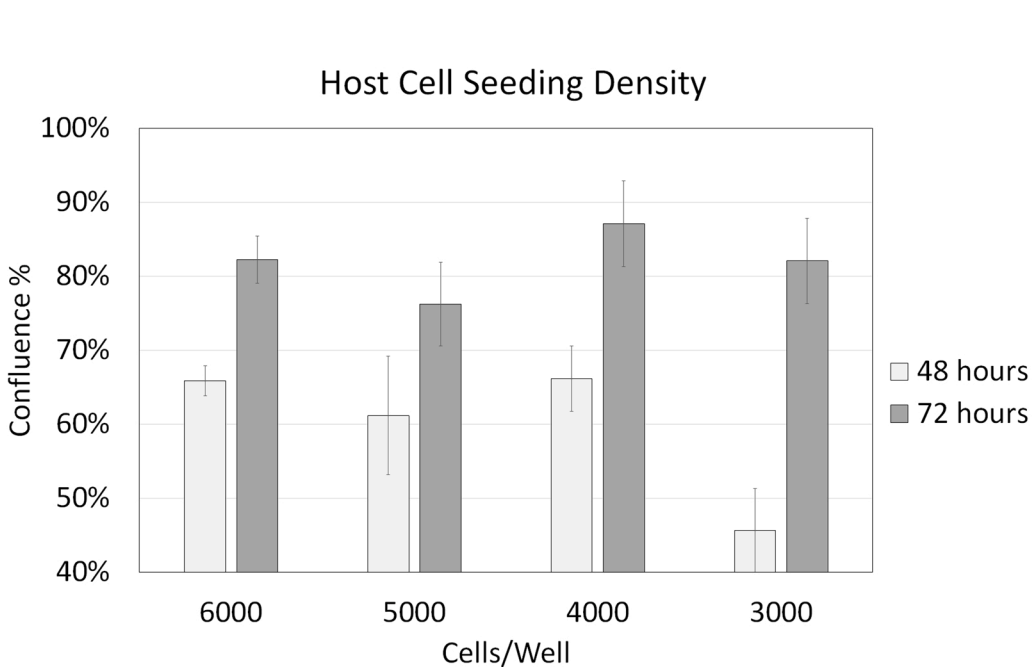

Fig. 2. Host cell seeding density and incubation time optimization results. (a) Bright field and confluence measurement overlay (pseudo-color green) for seeding densities 3000 – 6000 cells/well at 48 and 72 h showing coverage of CRFK cells on the well surface. (b) Time- and seeding density-dependent confluence percentages measured using image cytometry (For interpretation of the references to colour in this figure legend, the reader is referred to the web version of this article).

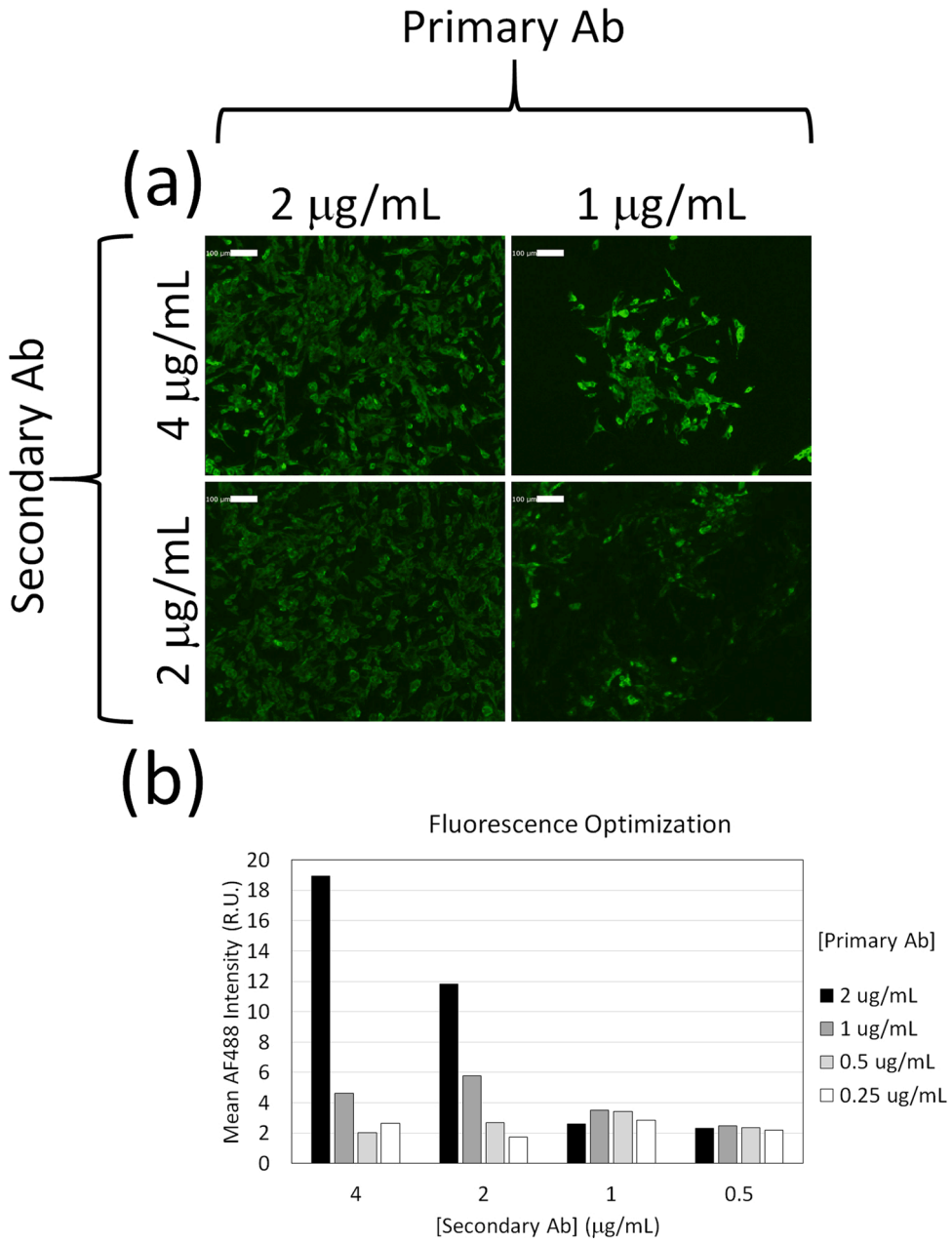

Fig. 3. Fluorescent labeling optimization results. (a) Fluorescent images of AF488-labeled infected CRFK cells showing green fluorescence for labeling with primary antibody at 1 and 2 µg/mL and secondary antibody at 2 and 4 µg/mL. (b) Mean AF488 fluorescence intensities measured using image cytometry (For interpretation of the references to colour in this figure legend, the reader is referred to the web version of this article).

Assessment of Laboratory Animal Care standards and with approval from the Colorado State University Institutional Animal Care and Use Committee (protocol 16-6390A, approved 11 July 2017). EDTA plasma of the type I FECV-infected cats was collected and stored at −80 °C as part of a previous study in which cats were monitored monthly for plasma FCoV antibodies and fecal FCoV RNA over seven months (Pearson et al., 2019). Five representative feline plasma samples (Table 1) were vortexed, centrifuged, and heat-inactivated at 57 °C for 1 h (Pearson et al., 2019). Next, 8 serial dilutions in DPBS were prepared directly in a 96-well titration plate (650201, Greiner Bio-One). The plasma samples were first diluted 1:10 in row "A" by adding 22 µL of plasma into 198 µL of DPBS (220 µL total) in triplicate. Rows "B" through "H" were then filled with 110 µL of DPBS, and subsequently, 110 µL of row "A" was added to row "B" and mixed. The procedure was repeated from rows "B" through "H" to generate the plasma dilutions of 1:20, 1:40, 1:80, 1:160, 1:320, 1:640, and 1:1280. The extra 110 µL at row "H" was discarded.

2.10. High-throughput FCoV microneutralization assay

The Celigo Image Cytometer was used to screen the selected plasma samples for neutralization of FCoV using the optimized assay parameters. First, 6000 CRFK cells per well were seeded in collagen type I-coated 96-well plates (655956, Greiner Bio-One) and cultured for 24 h. During this time, the viral supernatant (110 µL) at the optimal concentration (1:10 dilution of the viral stock solution in DPBS) was added to the 5 plasma samples in the prepared plasma titration plate described above and uniformly mixed with a multi-channel pipette. The plasma/virus mixtures were then incubated for at RT for 1 h. In addition, wells with only viral supernatant or only plasma were prepared as positive

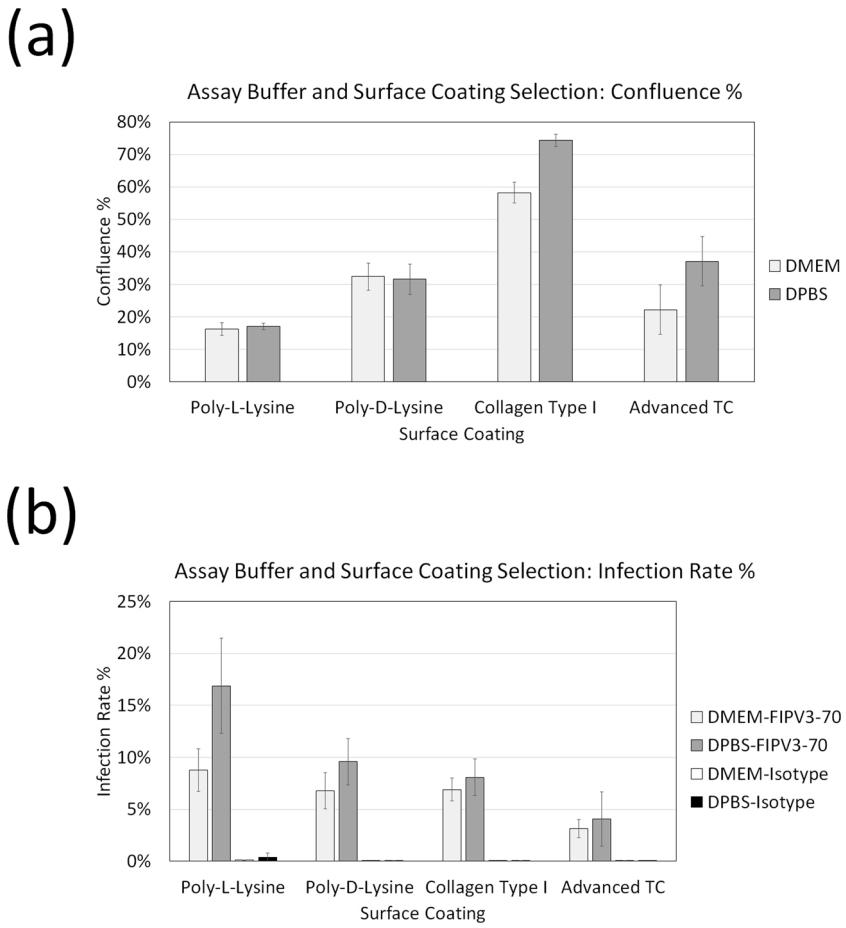

Fig. 4. Optimal assay buffer and surface coating selection results. Comparison of the CRFK (a) confluence percentages and (b) infection rates between DMEM and DPBS, as well as between Advanced TC, collagen type I, poly-D-lysine, and poly-L-lysine surface coating.

and negative controls.

During the plasma/virus incubation time, the host cell microplate was prepared by removing the CRFK medium and washing once with 200 µL of DPBS. After the plasma/viral supernatant incubation, the mixtures (100 µL) were added to the host cells and incubated for 1 h at 37 °C and 5% CO_2. After the incubation the plasma/virus mixtures were removed, the wells were washed 2X with 200 µL of DPBS. Next, 200 µL of CRFK medium was added to each well and the plates were incubated for 24 h. The infected cells were then fluorescently stained and immediately scanned and analyzed using the image cytometer.

3. Results

3.1. Optimization of the high-throughput image-based virus-infected cell detection assay

The scanning and analysis settings for every experiment were optimized to generate proper images and results (Fig. 1). The scanning parameters were selected to acquire bright field and fluorescent images that were in focus for the entire plate. The analysis parameters were selected so the software can accurately identify and count the total host cells and infected cells. After the settings were established, they were saved as experimental presets and applied to subsequent plates without the need for further adjustments.

Development of the image cytometry-based high-throughput FCoV infection detection method involved the optimization of key variables: host cell seeding density, fluorescent labeling, assay buffer, microplate surface coating, virus concentration, and incubation time. The first step in developing the method was to optimize the host cell seeding density. The seeding density-dependent bright field images and measured confluence percentages are shown in Fig. 2, which showed decreasing confluence as cell density decreased as expected. An optimal seeding density of 6000 cells per well and an incubation time of 48 h post-seeding allowed the host cells to reach approximately 66% confluence at the end of viral infection, where the cells can be fixed and stained for image cytometry analysis. Although the 72h time point showed cell confluence of 70% or higher, we observed that 72 h of incubation caused the host cells to form layers near the well edges that were easily washed off.

The acquired green fluorescent images at different primary and secondary antibody concentrations for antibody optimization are shown in Fig. 3a. Primary antibody at 2 µg/mL in combination with 2 or 4 µg/mL of secondary antibody generated uniform fluorescence bright enough for the Celigo software to count accurately. Similarly, the measured mean AF488 fluorescence intensities were higher with the same antibody concentrations (Fig. 3b). Although the AF488 fluorescence intensity was the highest at 4 µg/mL of the secondary antibody, the background fluorescence was measured by examining the cell-free well area, which was higher than at 2 µg/mL (data not shown). Therefore, 2 µg/mL was selected as the optimal concentration for both the primary and secondary antibodies. It was also determined that enumeration of CRFK cells required the use of a DAPI nuclear stain. While the Celigo can count many cell types by detection of cell edges in a bright field image, the contrast of the CRFK is too low to accurately identify individual cells in confluent areas. In addition, we observed that black-walled microplates reduced auto-fluorescence and light scattering near the edge of the wells and enabled 100% of the well to be included in the analysis, compared to less than 95% with clear plates

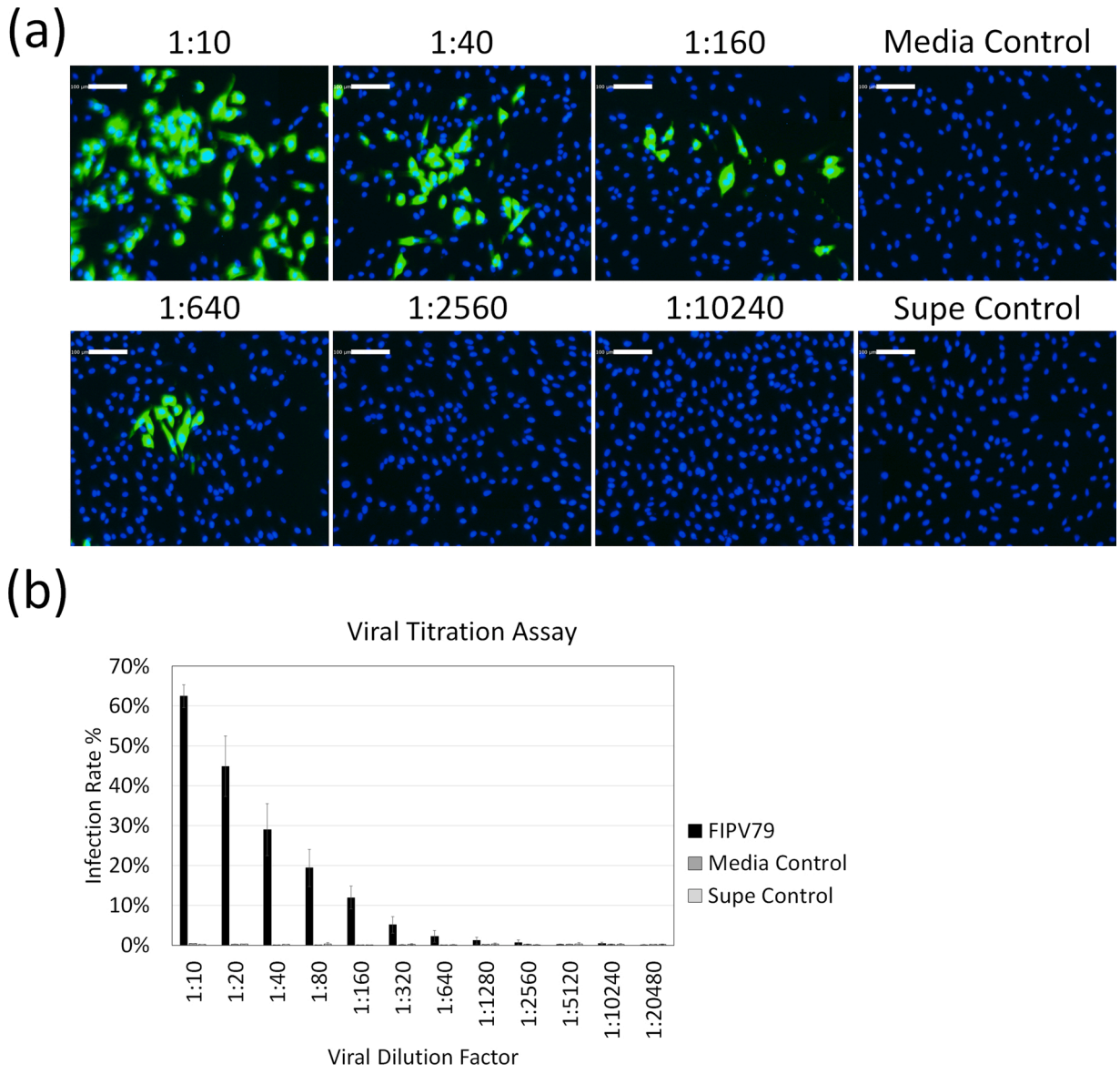

Fig. 5. Viral concentration optimization results. (a) Viral concentration-dependent fluorescent images and (b) infection rates measurement showing the reduction of AF488-positive infected CRFK cells as viral concentration decreased. Both media and supernatant control did not show viral infection.

(Supplementary Fig. 2).

Two assay buffers as well as four microplate surface coatings were compared by using the confluence analysis (Fig. 4a). DPBS demonstrated minimum cell loss during the wash and dilution steps, and the collagen type I surface coating allowed the highest adhesion of CRFK cells to the well surface. In addition, the infection rates were slightly higher with DPBS than with DMEM (Fig. 4b). It is important to note that the isotype control for the primary antibody showed no nonspecific cellular staining. The low number of infected cells counted in the DPBS-isotype wells represents the level of fluorescent artifact that could be used to establish the lower limit of quantification in viral titration assays (Fig. 4b).

The AF488 and DAPI overlay fluorescent images in respect to viral titration (Fig. 5a) show a decrease in virus-infected cells as viral concentrations decreased. The 1:10 dilution of viral stock solution yielded our desired 50–60% infected cells (Fig. 5b) and no infected cells were observed beyond 1:1280. The amount of cell loss during washing and staining steps increased at the 36, 48, and 72h time points. In order to minimize host cell loss during subsequent processing steps, a viral incubation time of 24 h was selected.

3.2. Feline plasma neutralization assay results

Five feline plasma samples were obtained from the Colorado State University closed cat colony, which had naturally circulating feline coronavirus in the population and was considered to be otherwise specific pathogen-free. The fluorescence-based high-throughput FCoV microneutralization assay was performed twice with the 5 plasma samples at 8 concentrations each in triplicates (Fig. 6). A high infection rate (50–90%) was measured and no infection was detected with only plasma. The plasma titrations showed no neutralization effects; however, the infection rates did show a slight inverse dose-dependent trend for each feline plasma.

4. Discussion

The high-throughput microneutralization assay described here represents an important advancement for the evaluation of vaccine candidates, testing of antiviral drugs, and investigation of FCoV pathogenesis. The method can easily be modified for other virological assays such as label-free cytolytic plaque counting, cytopathic effect detection, and

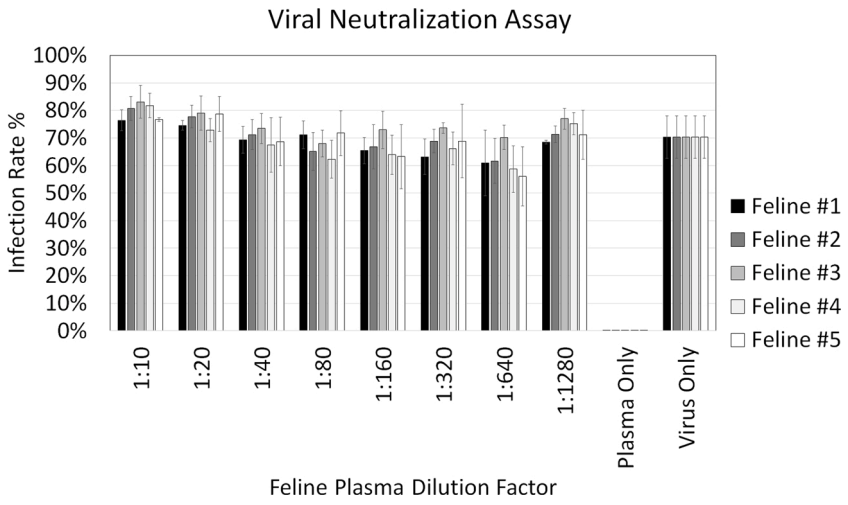

Fig. 6. Viral neutralization results showing dose-dependent infection rates measurements for 5 feline plasma samples with a titration from 1:10 to 1:1280. The virus and plasma only conditions showed high and low infection rates as expected. No noticeable neutralization effects were observed.

antibody-viral antigen binding inhibition assays (Masci et al., 2019; Rosen et al., 2019; Viedma and Pickett, 2018; Yang et al., 2017).

In this work, the development and optimization of the fluorescence-based virus-infected cell counting method was challenging due to the complex interactions of different variables. When optimizing the host cell seeding density, it was discovered that if the CRFK cells were not close to 60–70% confluency during the viral inoculation, the percentage of infected cells was inconsistent (data not shown). In addition, if confluency was greater than 70%, cells were more likely to lift off the well surface during subsequent processing steps. For the host cell seeding incubation, it was also important to select the shortest possible time frame after 24-h host cell adherence to minimize the assay time, as well as increase efficiency and throughput.

Filtration of the primary and secondary antibodies was determined to be beneficial; without filtration, fluorescent aggregation particles can be observed throughout the wells, which can cause nonspecific detection of infected cells. There were no differences observed between filtered and unfiltered DAPI. While it is possible to combine antigen and DAPI staining, we observed that the sequential staining of AF488 and DAPI generated stronger fluorescent signals.

It was observed that CRFK medium inhibited infection during the 1-h viral inoculation (data not shown), thus removing and washing the culture medium from the wells was critical. DPBS was selected for this step because it demonstrated minimal disruption to the adherence of the CRFK cells in comparison to DMEM. When washing with DMEM, most of the host cells lost adhesion to the bottom of the wells and disrupted their surface coverage. Therefore, DPBS was used for all wash steps as well as for the dilution of virus, plasma, and staining reagents.

The viral titer results revealed that the 50–60% infection rate optimal for the neutralization assay was achieved with a 1:10 dilution of the viral stock. A higher percentage could mask the neutralization effects, and a lower percentage could lead to more well-to-well variation. It is important to note that different dilutions of virus stock were used to optimize conditions for virus propagation and fluorescence testing.

After the optimization of each parameter for the high-throughput virus-infected cell counting method, the image cytometer performed the neutralization assay at approximately 15 min per 96-well plate for simultaneously acquiring and analyzing whole well images in bright field and fluorescence, equivalent to ~9 s per sample. The high-throughput functionality can be achieved with the developed method, allowing rapid screening for neutralizing antibodies in plasma or serum samples. In a 96-well plate, 11 columns may be dedicated to 11 samples at 8 dilutions, and the 12th column can be dedicated to positive and negative controls. Furthermore, the assay could be conducted in a 384-well plate to further increase the throughput of the screening assay.

The high-throughput neutralization assay was conducted two times and no FCoV neutralization was observed; however, the lack of neutralization was not surprising. The virus used in this assay, FCoV-WSU- 79-1146, is a type II virus while the cats evaluated in this study were infected with a type I FECV (Pearson et al., 2019). The spike proteins of type I and II viruses differ significantly in sequence, structure and function (Jaimes et al., 2020). Furthermore, while feline aminopeptidase N (fAPN) is known to be the target cell receptor used by type II viruses, the type I receptor remains unknown (Dye et al., 2007; Hohdatsu et al., 1998). These differences explain why antibodies against either serotype may not cross-neutralize (Pedersen et al., 1984; Terada et al., 2014). Unfortunately, type I viruses do not readily grow in cell culture, which creates an obstacle to assessment of antibody neutralization in an appropriate homologous assay format using plasma from type I infected cats against type I virus infection in vitro. Recent advances that may eventually address this conundrum include the generation of an infectious type I molecular clone and knock-out of the type I alpha-interferon receptor 1 in feline cells (Mettelman et al., 2019; Terada et al., 2019). The latter may allow more robust replication of natural type I FECV isolates.

The use of the Celigo Image Cytometer reduces assay time while providing richer, quantitative readouts to accelerate assessment of vaccine and antiviral compound candidates. Importantly, the optimization strategy can be employed to adapt other cell types to the assay format or to create entirely new virus-host cell combinations.

CRediT authorship contribution statement

Morgan Pearson: Conceptualization, Data curation, Formal analysis, Investigation, Methodology, Project administration, Writing - original draft, Writing - review & editing. **Alora LaVoy:** Conceptualization, Data curation, Formal analysis, Investigation, Methodology, Writing - original draft, Writing - review & editing. **Leo Li-Ying Chan:** Conceptualization, Formal analysis, Methodology, Visualization, Writing - original draft, Writing - review & editing. **Gregg A. Dean:** Conceptualization, Methodology, Project administration, Writing - original draft, Writing - review & editing.

Declaration of Competing Interest

The author LLC declares competing financial interests. The research instrument used in this manuscript is a product of Nexcelom Bioscience, LLC. The work was performed to demonstrate a novel high-throughput

viral neutralization screening method for feline coronavirus using the Celigo Image Cytometer.

Acknowledgment

The authors wish to acknowledge the support of the Morris Animal Foundation award #D17FE-009. The author, MP, was supported by NIH Grant Number T32 OD01220.

Appendix A. Supplementary data

Supplementary material related to this article can be found, in the online version, at doi:https://doi.org/10.1016/j.jviromet.2020.113979.

References

Addie, D., Belák, S., Boucraut-Baralon, C., Egberink, H., Frymus, T., Gruffydd-Jones, T., Hartmann, K., Hosie, M.J., Lloret, A., Lutz, H., Marsilio, F., Pennisi, M.G., Radford, A.D., Thiry, E., Truyen, U., Horzinek, M.C., 2009. Feline infectious peritonitis. ABCD guidelines on prevention and management. J. Feline Med. Surg. 11, 594–604.

Addie, D.D., Curran, S., Bellini, F., Crowe, B., Sheehan, E., Ukrainchuk, L., Decaro, N., 2020. Oral Mutian®X stopped faecal feline coronavirus shedding by naturally infected cats. Res. Vet. Sci. 130, 222–229.

An, D.-J., Jeoung, H.-Y., Jeong, W., Park, J.-Y., Lee, M.-H., Park, B.-K., 2011. Prevalence of Korean cats with natural feline coronavirus infections. Virol. J. 8 https://doi.org/10.1186/1743-422X-8-455.

Chan, L.L.-Y., 2020. High-Throughput Direct Cell Counting Method for Immuno-Oncology Functional Assays Using Image Cytometry. In: Tan, S.-L. (Ed.), Immuno-Oncology: Cellular and Translational Approaches. Springer US.

Dickinson, P.J., Bannasch, M., Thomasy, S.M., Murthy, V.D., Vernau, K.M., Liepnieks, M., Montgomery, E., Knickelbein, K.E., Murphy, B., Pedersen, N.C., 2020. Antiviral treatment using the adenosine nucleoside analogue GS -441524 in cats with clinically diagnosed neurological feline infectious peritonitis. J. Vet. Intern. Med. https://doi.org/10.1111/jvim.15780.

Dye, C., Temperton, N., Siddell, S.G., 2007. Type I feline coronavirus spike glycoprotein fails to recognize aminopeptidase N as a functional receptor on feline cell lines. J. Gen. Virol. 88, 1753–1760.

Felten, S., Hartmann, K., 2019. Diagnosis of feline infectious peritonitis: a review of the current literature. Viruses 11, 1068.

Foley, J.E., Lapointe, J.-M., Koblik, P., Poland, A., Pedersen, N.C., 1998. Diagnostic features of clinical neurologic feline infectious peritonitis. J. Vet. Intern. Med. 12, 415–423.

Hartmann, K., 2005. Feline infectious peritonitis. Vet. Clin. North Am. Small Anim. Pract. 35, 39–79.

Herrewegh, A.A.P.M., Smeenk, I., Horzinek, M.C., Rottier, P.J.M., Groot, R.Jd., 1998. Feline coronavirus type II strains 79-1683 and 79-1146 originate from a double recombination between feline coronavirus type I and canine coronavirus. J. Virol. 72, 4508–4514.

Hohdatsu, T., Izumiya, Y., Yokoyama, Y., Kida, K., Koyama, H., 1998. Differences in virus receptor for type I and type II feline infectious peritonitis virus. Arch. Virol. 143, 839–850.

Jaimes, J.A., Millet, J.K., Stout, A.E., André, N.M., Whittaker, G.R., 2020. A tale of two viruses: the distinct Spike Glycoproteins of feline coronaviruses. Viruses 12, 83.

Jorquera, P.A., Mishin, V.P., Chesnokov, A., Nguyen, H.T., Mann, B., Garten, R., Barnes, J., Hodges, E., Cruz, J.D.L., Xu, X., Katz, J., Wentworth, D.E., Gubareva, L.V., 2019. Insights into the antigenic advancement of influenza A(H3N2) viruses, 2011–2018. Sci. Rep. 9 https://doi.org/10.1038/s41598-019-39276-1.

Kessel, S., Cribbes, S., Déry, O., Kuksin, D., Sincoff, E., Qiu, J., Chan, L.L.-Y., 2016. High-throughput 3D tumor spheroid screening method for Cancer drug discovery using celigo image cytometry. J. Lab. Autom. https://doi.org/10.1177/2211068216652846.

Kummrow, M., Meli, M.L., Haessig, M., Goenczi, E., Poland, A., Pedersen, N.C., Hofmann-Lehmann, R., Lutz, H., 2005. Feline coronavirus serotypes 1 and 2: seroprevalence and association with disease in Switzerland. Clin. Diagn. Lab. Immunol. 12, 1209–1215.

Li, F., 2016. Structure, function, and evolution of coronavirus spike proteins. Annu. Rev. Virol. 3, 237–261.

Masci, A.L., Menesale, E.B., Chen, W.-C., Co, C., Lu, X., Bergelson, S., 2019. Integration of fluorescence detection and image-based automated counting increases speed, sensitivity, and robustness of plaque assays. Mol. Ther. Methods Clin. Dev. 14, 270–274.

Mettelman, R.C., O'Brien, A., Whittaker, G.R., Baker, S.C., 2019. Generating and evaluating type I interferon receptor-deficient and feline TMPRSS2-expressing cells for propagating serotype I feline infectious peritonitis virus. Virology 537, 226–236.

Pearson, M., LaVoy, A., Evans, S., Vilander, A., Webb, C., Graham, B., Musselman, E., LeCureux, J., VandeWoude, S., Dean, G.A., 2019. Mucosal immune response to feline enteric coronavirus infection. Viruses 11, 906.

Pedersen, N.C., 2014a. An update on feline infectious peritonitis: diagnostics and therapeutics. Vet. J. 201, 133–141.

Pedersen, N.C., 2014b. An update on feline infectious peritonitis: virology and immunopathogenesis. Vet. J. 201, 123–132.

Pedersen, N.C., Evermann, J.F., McKeirnan, A.J., Ott, R.L., 1984. Pathogenicity studies of feline coronavirus isolates 79-1146 and 79-1683. Am. J. Vet. Res. 45, 2580–2585.

Pedersen, N.C., Perron, M., Bannasch, M., Montgomery, E., Murakami, E., Liepnieks, M., Liu, H., 2019. Efficacy and safety of the nucleoside analog GS-441524 for treatment of cats with naturally occurring feline infectious peritonitis. J. Feline Med. Surg. 21, 271–281.

Pratelli, A., 2008. Comparison of serologic techniques for the detection of antibodies against feline coronaviruses. J. Vet. Diagnost. Investiv. 20, 45–50.

Ramos, I., Smith, G., Ruf-Zamojski, F., Martínez-Romero, C., Fribourg, M., Carbajal, E.A., Hartmann, B.M., Nair, V.D., Marjanovic, N., Monteagudo, P.L., DeJesus, V.A., Mutetwa, T., Zamojski, M., Tan, G.S., Jayaprakash, C., Zaslavsky, E., Albrecht, R.A., Sealfon, S.C., García-Sastre, A., Fernandez-Sesma, A., 2019. Innate immune response to influenza virus at single-cell resolution in human epithelial cells revealed paracrine induction of interferon lambda 1. J. Virol. 93, e00559–19.

Rohrbach, B.W., Legendre, A.M., Baldwin, C.A., Lein, D.H., Reed, W.M., Wilson, R.B., 2001. Epidemiology of feline infectious peritonitis among cats examined at veterinary medical teaching hospitals. J. Am. Vet. Med. Assoc. 218, 1111–1115.

Rosen, O., Chan, L.L.-Y., Abiona, O.M., Gough, P., Wang, L., Shi, W., Zhang, Y., Wang, N., Kong, W.-P., McLellan, J.S., Graham, B.S., Corbett, K.S., 2019. A high-throughput inhibition assay to study MERS-CoV antibody interactions using image cytometry. J. Virol. Methods 265, 77–83.

Shambaugh, C., Azshirvani, S., Yu, L., Pache, J., Lambert, S.L., Zuo, F., Esser, M.T., 2017. Development of a high-throughput respiratory syncytial virus fluorescent focus-based microneutralization assay. Clin. Vaccine Immunol. 24 e00225-17.

Shiba, N., Maeda, K., Kato, H., Mochizuki, M., Iwata, H., 2007. Differentiation of feline coronavirus type I and II infections by virus neutralization test. Vet. Microbiol. 124, 348–352.

Takano, T., Satoh, K., Doki, T., Tanabe, T., Hohdatsu, T., 2020. Antiviral effects of Hydroxychloroquine and type I interferon on in vitro fatal feline coronavirus infection. Viruses 12, 576.

Terada, Y., Matsui, N., Noguchi, K., Kuwata, R., Shimoda, H., Soma, T., Mochizuki, M., Maeda, K., 2014. Emergence of pathogenic coronaviruses in cats by homologous recombination between feline and canine coronaviruses. PLoS One 9, e106534.

Terada, Y., Kuroda, Y., Morikawa, S., Matsuura, Y., Maeda, K., Kamitani, W., 2019. Establishment of a virulent full-length cDNA clone for type I feline coronavirus strain C3663. J. Virol. 93, e01208–19.

Viedma, Md.P.M., Pickett, B.E., 2018. Characterizing the different effects of zika virus infection in Placenta and microglia cells. Viruses 10, E649.

Whittaker, G.R., André, N.M., Millet, J.K., 2018. Improving virus taxonomy by recontextualizing sequence-based classification with biologically relevant data: the case of the alphacoronavirus 1 species. mSphere 3, e00463–17.

Yang, M.-L., Wang, C.-T., Yang, S.-J., Leu, C.-H., Chen, S.-H., Wu, C.-L., Shiau, A.-L., 2017. IL-6 ameliorates acute lung injury in influenza virus infection. Sci. Rep. 7 https://doi.org/10.1038/srep43829.

Zhang, H., Chan, L.L.-Y., Rice, W., Kassam, N., Longhi, M.S., Zhao, H., Robson, S.C., Gao, W., Wu, Y., 2017. Novel high-throughput cell-based hybridoma screening methodology using the Celigo Image Cytometer. J. Immunol. Methods 447, 23–30.